Optic-phonon-limited transport and anomalous carrier cooling in quantum-wire structures

J. P. Leburton
Beckman Institute for Advanced Science and Technology, Department of Electrical and Computer Engineering, University of Illinois at Urbana-Champaign, Urbana, Illinois 61801
(Received 21 October 1991)

We present an analytical derivation of the distribution function of a one-dimensional electron gas at high temperature. The quenching of carrier-carrier scattering and the predominance of polar-optic-phonon scattering make the system nonergodic and provide a "jagged" profile to the distribution which results in carrier cooling below the thermal energy. In GaAs quantum wires, this anomalous effect, which is characterized by extremely high carrier mobility, is predicted to occur above $T_L = 150$ K. These conclusions are in excellent agreement with results of Monte Carlo simulations.

I. INTRODUCTION

In the past few years, the physics of reduced dimensionality systems has experienced a rapid development, mainly stimulated by the considerable advance in fine-line lithography and crystal-growth techniques.[1-6] Quasi-one-dimensional (1D) systems, or quantum wires, have recently been investigated for the transport properties associated with universal conductance fluctuations and quantum interference phenomena.[7] At high temperature, however, strong phonon scattering prohibits long-range coherence arising from the wave nature of the electrons, and carrier motion can be described in terms of particle dynamics. In this context the transport properties of 1D systems are essentially different from 2D and 3D systems.[8] Among other factors, the reduction of momentum space to a single dimension (even with multiple transverse modes), has profound consequences on carrier statistics because it limits the number of available final scattering states.[9] Significant mobility enhancement has been predicted for both low- (Ref. 10) and high-temperature 1D transport.[11] Detailed Monte Carlo simulation of hot 1D carrier transport at room temperature shows significant deviations from the Maxwellian distribution at intermediate electric fields ($F \sim 100$ V/cm) (Ref. 12). Pronounced structures at multiples of the longitudinal-optic (LO) polar-optic-phonon (POP) energy $E = n\hbar\omega$ are predicted in the distribution function (DF) which exhibits a "jagged" profile once POP absorption is appreciable, i.e., above $T = 100$ K.[13] It has been shown in previous works that this singular behavior is enhanced in the case of resonances between the POP energy and the 1D subband separation,[14] and induced population inversion between adjacent off-resonance subbands.[15] Although these effects have only been established by numerical simulations, the existence of non-Maxwellian jagged DF compatible with the Boltzmann equation has not yet been demonstrated. In this paper, we derive an analytical solution of the Boltzmann equation which is consistent with Monte Carlo simulation. More than providing a confirmation of earlier numerical results, our analysis reexamines the popular concept of Maxwell distribution[16] and the ergodicity of 1D systems in the presence of POP scattering. In particular, we show that the 1D carrier mobility can exceed its bulk value by almost an order of magnitude at room temperature, and the electron system undergoes a cooling below the thermal energy.

II. ELECTRONIC PROPERTIES AND SCATTERING RATES

In this analysis we assume that simple confinement configurations in quantum wires arise from elementary GaAs-$Al_xGa_{1-x}As$ potential wells which are decoupled along the two transverse y and z directions. Electrons are free to move along the x direction with energies and wave functions given by

$$E_{ij}(k_x) = \frac{\hbar^2 k_x^2}{2m} + E_i + E_j \quad \text{with } i,j = 1, \ldots, N \tag{1}$$

and

$$\psi_{ij}(k_x, \mathbf{r}) = \frac{1}{\sqrt{L_x}} e^{ik_x x} \xi_i(y) \phi_j(z) , \tag{2}$$

where k_x and L_x are the wave vector and the wire length in the longitudinal direction and $\xi_i(y)$ and $\phi_j(z)$ are the transverse wave functions which correspond to the quantized energy levels E_i and E_j, respectively. N is the maximum number of levels considered in a particular confinement situation. The remaining term in Eq. (1) is the kinetic energy of the particle resulting from the free-electron component of the overall electronic wave function [Eq. (2)]. The advantage of dealing with elementary configuration is the decoupling of the electronic y and z wave functions, which facilitates the computation of the scattering rates.

In modulation-doped GaAs structures, ionized-impurity (II) scattering is insignificant at high temperature, and acoustic-phonon (AP) scattering ($\tau_{ac}^{-1} \approx 10^{10-11}$ s^{-1}) becomes inefficient compared to POP scattering ($\tau_{POP}^{-1} \geq 10^{12}$ s^{-1}) once electric fields F significantly exceeds 10 V/cm.[17] In addition, carrier-carrier scattering vanishes for *intrasubband* binary processes. From the 1D conservation laws, one obtains

 ©1992 The American Physical Society

$$\frac{p_1^2}{2m}+\frac{p_2^2}{2m}=\frac{p_1'^2}{2m}+\frac{p_2'^2}{2m}\ , \tag{3a}$$

$$p_1+p_2=p_1'+p_2'\ , \tag{3b}$$

where p_1, p_2 and p_1',p_2' are the 1D electron momenta, respectively, before and after interaction. It can be seen that carriers simply exchange energies and momenta during collisions. For indistinguishable particles, this process is irrelevant.[12] Consequently, intrasubband thermalization is suppressed. Therefore, electron-POP interaction is the only mechanism for carrier-energy dissipation and momentum randomization. The general form of the electron-phonon Hamiltonian reads[18]

$$H_{e\text{-ph}}=\sum_{\mathbf{q}} C_{\mathbf{q}}(a_{\mathbf{q}}e^{i\mathbf{q}r}-a_{\mathbf{q}}^{\dagger}e^{-i\mathbf{q}r})\ , \tag{4}$$

where $a_{\mathbf{q}}^{\dagger}$ and $a_{\mathbf{q}}$ are the phonon creation and annihilation operators and $C_{\mathbf{q}}$ determines the electron-phonon coupling strength given by[19]

$$C_{\mathbf{q}}=-i\left[\frac{2\pi}{\mathrm{Vol}}e^2\hbar\omega\left(\frac{1}{\epsilon_\infty}-\frac{1}{\epsilon_0}\right)\right]^{1/2}\frac{1}{q}\ . \tag{5}$$

Here Vol is the wire volume and ϵ_∞ and ϵ_0 are the optical and static dielectric constants, respectively. ω ($\cong$36 meV) is the POP frequency. The $1/q$ dependence of $C_{\mathbf{q}}$ implies that collisions involving small exchanges of momentum are the most favorable for the POP interaction. Although recent work has demonstrated the importance of treating confined phonon modes in highly quantized systems,[20] only bulk modes are treated here. This is a good approximation as long as well widths are not narrower than 50 Å.

In the semiclassical limit, the expression, for the 1D transition probability $S_{\nu\nu'}(k_x,k_x')$ derived from Fermi's golden rule, reads

$$S_{\nu\nu'}(k_x,k_x')=\frac{2\pi}{\hbar}\sum_{\mathbf{q}_\perp}|M_{\nu\nu'}(k_x,k_x';\mathbf{q})|^2 \times\delta[E_{\nu'}'(k_x')-E_\nu(k_x)\pm\hbar\omega]\ , \tag{6}$$

with

$$M_{\nu\nu'}(k_x,k_x';\mathbf{q})=(N_q+\tfrac{1}{2}\pm\tfrac{1}{2})^{1/2}C_{\mathbf{q}}\delta_{k_x k_x'\pm q_x} \times\int dy\,\xi_i^{*\prime}(y)\xi_i(y)e^{\pm iq_y y} \times\int dz\,\phi_i'^{*}(z)\phi_j(z)e^{\pm iq_z z}\ . \tag{7}$$

The indices i, i', j, and j' refer to the quantum numbers of the transverse wave functions which together determine the subband indices ν and ν'. $M(k_x,k_x';\mathbf{q})$ represents the electron-phonon matrix elements for a transition from an initial k_x,ν state to the final k_x',ν' state mediated by a phonon with wave vector $\mathbf{q}$. This matrix element is summed up over all transverse components $\mathbf{q}_\perp$ to provide the 1D transition probability. The $\pm$ sign in the prefactor of Eq. (7), and the energy-conserving δ function [Eq. (6)], account for emission (+) and absorption (−) of phonons between subbands with indices $\nu'(i',j')$ and $\nu(i,j)$. We can transform the energy δ function into wave-vector-conserving δ functions and obtain

$$\delta[E_{\nu'}'(k_x')-E_\nu(k_x)\pm\hbar\omega] =\frac{m}{\hbar^2K_{\nu\nu'}^{\mp}}[\delta(k_x'-K_{\nu\nu'}^{\mp})+\delta(k_x'+K_{\nu\nu'}^{\mp})]\ , \tag{8}$$

with

$$K_{\nu\nu'}^{\pm}=\left[\frac{2m}{\hbar^2}(E_\nu-E_{\nu'}\pm\hbar\omega)+k_x^2\right]^{1/2} \tag{9}$$

and

$$E_\nu=E_i+E_j\ , \tag{10a}$$

$$E_\nu(k_x)=E_\nu+\frac{\hbar^2k_x^2}{2m}\ , \tag{10b}$$

and similarly for $E_{\nu'}(k_x')$.

If we call backward (forward) scattering events which do (not) reverse the carrier momentum, the first term on the right-hand side (RHS) of Eq. (8) corresponds to forward (f) [backward (b)] scattering if k_x is positive (negative). The second term corresponds to backward (b) [forward (f)] for the same condition (Fig. 1). The transition probability becomes

$$S_{\nu\nu'}(k_x-k_x')=I_{\nu\nu'}^{\mp}(|k_x-k_x'|)[\delta(k_x'-K_{\nu\nu'}^{\mp}) +\delta(k_x'+K_{\nu\nu'}^{\mp})]\ , \tag{11}$$

with

$$I_{\nu\nu'}^{\mp}(|k_x-k_x'|)=\frac{2\pi}{\hbar}\sum_{\mathbf{q}_\perp}|M_{\nu\nu'}(k_x,k_x';\mathbf{q})|^2\frac{m}{\hbar^2K_{\nu\nu'}^{\mp}} \tag{12}$$

and depends on the absolute value of $q_x=k_x-k_x'$ since $C_{\mathbf{q}}$ is proportional to $1/|\mathbf{q}|$. In particular, if we consider

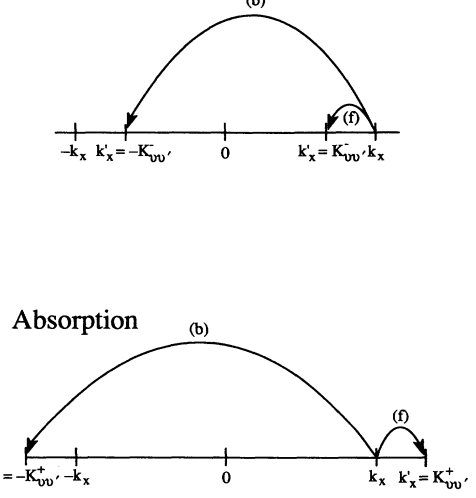

FIG. 1. Schematics representing the four fundamental POP scattering processes in 1D systems POP emission and POP absorption with both forward and backward processes from an initial k_x state to a final k_x' state.

only the lowest subband and neglect intersubband transitions $\nu=\nu'=(1,1)$,

$$S_{11}(k_x-k_x')=S_{(a,e)}(|k_x-k_x'|) =I^{\mp}_{(a,e)}(|k_x-k_x'|) \times[\delta(k_x'-K^{\mp})+\delta(k_x'+K^{\mp})] , \quad (13)$$

with

$$K^{\mp}=\left[k_x^2\mp\frac{2m\omega}{\hbar}\right]^{1/2} . \quad (14)$$

Here, the subscripts a and e stand for phonon absorption and emission, respectively. The total scattering rate from an initial state with energy $E(k_x)$ is given by

$$\lambda_\nu[E(k_x)]=\sum_{k_x',\nu'} S_{\nu\nu'}(k_x,k_x') . \quad (15)$$

The summation over the final states k_x',ν' takes into account all possible forward (f) and backward (b) intersubband transitions along with those occurring within the same subband ν.

III. BOLTZMANN EQUATION

In the following, we will assume that we deal with a nondegenerate electron gas interacting with POP's only. In order to simplify the analysis, we consider the extreme quantum limit, i.e., where only the lowest subband is occupied, and neglect intersubband transitions which would considerably complicate our derivation without introducing new physical effects. Such a situation arises in extremely confined 1D systems as in field-effect transistor quantum wires realized with a V-groove structure, with moderate longitudinal electric fields ($F\lesssim 500$ V/cm) to prevent electron excitation to the upper subbands.

In steady-state and spatially homogeneous systems, the Boltzmann equation takes the following form:

$$\frac{eF}{\hbar}\frac{d}{dk_x}f^{\pm}(k_x)=-f^{\pm}(k_x)\sum_{k_x'}[S_a^f(k_x-k_x')+S_a^b(k_x-k_x')+S_e^f(k_x-k_x')+S_e^b(k_x-k_x')] + \sum_{k_x'}[S_a^f(k_x'-k_x)f^{\pm}(k_x')+S_a^b(k_x'-k_x)f^{\mp}(k_x')+S_e^f(k_x'-k)f^{\pm}(k_x')+S_e^b(k_x'-k)f^{\mp}(k_x')] , \quad (16)$$

where $f^{\pm}(k_x)$ is the distribution function for momentum $\hbar k_x=\pm\sqrt{2mE}$ and the superscripts identify the f- and b-scattering processes. The first sum on the RHS of Eq. (16) corresponds to outscattering events involving all POP a, e, f, and b processes. The second sum corresponds to all POP inscattering events. Because of the energy conservation (δ function in the S terms) the summation over k_x' is reduced to only one term, i.e.,

$$\frac{eF}{\hbar}\frac{d}{dk_x}f^{\pm}(k_x)=-\frac{L_x}{2\pi}[I_a^f(k_x\mp K^+)+I_a^b(k_x\pm K^+)+I_e^f(k_x\mp K^-)+I_e^b(k_x\pm K^-)]f^{\pm}(k_x) +\frac{L_x}{2\pi}[I_a^f(K^-\mp k_x)f^{\pm}(K^-)+I_a^b(K^-\pm k_x)f^{\mp}(K^-)+I_e^f(K^+\mp k_x)f^{\pm}(K^+)+I_e^b(K^+\pm k_x)f^{\mp}(K^+)] , \quad (17)$$

where L_x is the wire length.

From Eqs. (13) and (14) [since $I(|k_x-k_x'|)$ only depends on the absolute value of the difference between the two wave vectors] we notice that

$$\frac{L_x}{2\pi}\frac{I_a^f(k_x\mp K^+)}{N_q}=\frac{L_x}{2\pi}\frac{I_e^f(K^+\mp k_x)}{1+N_q}=\frac{1}{\tau_+^f} , \quad (18a)$$

$$\frac{L_x}{2\pi}\frac{I_a^b(k_x\pm K^+)}{N_q}=\frac{2\pi}{L_x}\frac{I_e^b(K^+\pm k_x)}{1+N_q}=\frac{1}{\tau_+^b} , \quad (18b)$$

where the $\pm$ sign is for k_x positive or negative, respectively. We obtain similar expressions with K^- that we call $1/\tau_-^f$ and $1/\tau_-^b$, respectively. By changing variables and setting $E=\hbar^2k_x^2/2m$, Eq. (17) reads

$$\pm eF\left[\frac{2E}{m}\right]^{1/2}\frac{d}{dE}f^{\pm}(E)=-\left[\frac{1+N_q}{\tau_-}+\frac{N_q}{\tau_+}\right]f^{\pm}(E)+(1+N_q)\left[\frac{f^{\pm}(E+\hbar\omega)}{\tau_+^f}+\frac{f^{\mp}(E+\hbar\omega)}{\tau_+^b}\right] +N_q\left[\frac{f^{\pm}(E-\hbar\omega)}{\tau_-^f}+\frac{f^{\mp}(E-\hbar\omega)}{\tau_-^b}\right] , \quad (19)$$

where the bare POP rate (i.e., without the phonon occupation numbers $1+N_q$ and N_q) can be written as

$$\frac{1}{\tau_{\pm}^{f,b}}=\frac{1}{\tau_{0\pm}^{f,b}(E)}\frac{1}{\left[\frac{E}{\hbar\omega}\pm 1\right]^{1/2}}\ . \tag{20}$$

The square root accounts for the profile of the 1D density of states and $1/\tau_0^{f,b}$ is a form factor containing the 3D phonon matrix element

$$\frac{1}{\tau_{0\pm}^{f,b}(E)}=\frac{\mathrm{Vol}}{(2\pi)^2}\frac{1}{\hbar^2}\left[\frac{m}{2\hbar\omega}\right]^{1/2}\times\int d_{q_\perp}|M(|k_x\pm K^{\pm}|;q_\perp)|^2\ , \tag{21}$$

where Vol is the wire volume. From the total scattering rate, we have also the relation

$$\frac{1}{\tau_{\pm}}=\frac{1}{\tau_{\pm}^{f}}+\frac{1}{\tau_{\pm}^{b}}\ , \tag{22}$$

with

$$\frac{1}{\tau_{0\pm}}=\frac{1}{\tau_{0\pm}^{f}}+\frac{1}{\tau_{0\pm}^{b}}\ , \tag{23}$$

which yield the useful relation

$$\frac{1}{\tau_{0+}^{f,b}(E)}=\frac{1}{\tau_{0-}^{f,b}(E+\hbar\omega)}\ . \tag{24}$$

In Fig. 2, we show the total POP scattering rate for absorption and emission with f and b contributions for the ground subband of a quantum wire formed at the heterojunction of a V-groove structure[10] with a quantum well of 135-Å well width and a triangular confining potential with $F=120$ kV/cm.[11]

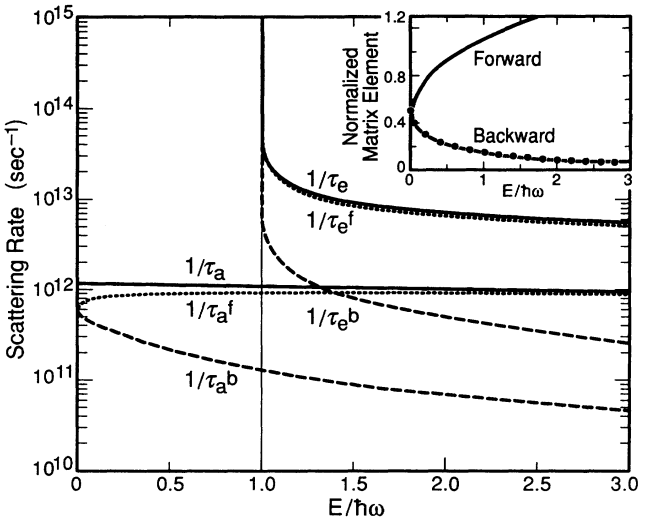

FIG. 2. Total POP scattering rate for the confinement conditions described in the text. The influence of upper subbands are omitted solid lines. Total emission ($1/\tau_e$) and absorption ($1/\tau_a$) rates, respectively; dot lines denote forward (f) processes; dashed lines denote backward (b) processes. Inset shows normalized matrix element $1/\tau_0$ for electron-POP interaction summed over the transverse POP wave vectors. Upper curve represents forward scattering; lower curve represents backward scattering; dots denote expression $(1/2)[1-\sqrt{E/(E+\hbar\omega)}]$ used in Eq. (37).

IV. SOLUTION OF THE BOLTZMANN EQUATION

Because of the discrete nature of optic phonons, POP scattering redistributes carrier energy between the intervals $n\hbar\omega\le E\le(n+1)\hbar\omega$ with $n=0,1,2,\ldots$, etc. without causing *intrainterval* randomization. Moreover, as we emphasized in Sec. II, intercarrier scattering is absent in the single-subband process, so carriers cannot thermalize. Thus, the system is not ergodic at equilibrium, since particles are unable to cover all points in phase space.[21] In these conditions the DF function has no *a priori* specific profile reminiscent of the Maxwellian distribution, as would be expected from the linear-response theory, or the electron-temperature model.[16] In the first-energy interval $0\le E\le\hbar\omega$, POP emission and inscattering absorption are prohibited, so Eq. (19) reads[12]

$$\frac{d}{dE}f^{\pm}(E)=\mp\frac{N_q}{W_+(E)}f^{\pm}(E)\pm(1+N_q)\times\left[\frac{f^{\pm}(E+\hbar\omega)}{W_+^{f}(E)}+\frac{f^{\mp}(E+\hbar\omega)}{W_+^{b}(E)}\right] \tag{25}$$

for $0\le E\le\hbar\omega$, and

$$\frac{d}{dE}f^{\pm}(E)=\mp\left[\frac{1+N_q}{W_-(E)}+\frac{N_q}{W_+(E)}\right]f^{\pm}(E)\pm(1+N_q)\times\left[\frac{f^{\pm}(E+\hbar\omega)}{W_+^{f}(E)}+\frac{f^{\mp}(E+\hbar\omega)}{W_+^{b}(E)}\right]\pm N_q\left[\frac{f^{\pm}(E-\hbar\omega)}{W_-^{f}(E)}+\frac{f^{\mp}(E-\hbar\omega)}{W_-^{b}(E)}\right] \tag{26}$$

for $n\hbar\omega\le E\le(n+1)\hbar\omega$ and $n\ge 1$, with

$$W_{\pm}^{f,b}(E)=eF\left[\frac{2E}{m}\right]^{1/2}\tau_{0\pm}^{f,b}(E)\left[\frac{E}{\hbar\omega}\pm 1\right]^{1/2}\ , \tag{27}$$

which obeys the relation $W_+^{f,b}(E-\hbar\omega)=W_-^{f,b}(E)$ [see Eq. (24)]. We can translate Eq. (26) into the energy interval $0\le E\le\hbar\omega$, by the transformation $E\to E+n\hbar\omega$, and obtain

$$\frac{d}{dE}f^{\pm}(E+n\hbar\omega)=\mp\left[\frac{1+N_q}{W_-(E+n\hbar\omega)}+\frac{N_q}{W_+(E+n\hbar\omega)}\right]f^{\pm}(E+n\hbar\omega)$$
$$\pm(1+N_q)\left[\frac{f^{\pm}[E+(n+1)\hbar\omega]}{W_+^f(E+n\hbar\omega)}+\frac{f^{\mp}[E+(n+1)\hbar\omega]}{W_+^b(E+n\hbar\omega)}\right]$$
$$\pm N_q\left[\frac{f^{\pm}[E+(n-1)\hbar\omega]}{W_-^f(E+n\hbar\omega)}+\frac{f^{\mp}[E+(n-1)\hbar\omega]}{W_-^b(E+n\hbar\omega)}\right] \tag{28}$$

for $n=0,1,2,\ldots$, etc. The first term within the first set of large parentheses and the two terms within the last set of large parentheses on the RHS vanish for $n=0$.

Let us define the symmetric f_s and antisymmetric f_a parts of the distribution function:

$$f_s^n(E)=\tfrac{1}{2}[f^+(E+n\hbar\omega)+f^-(E+n\hbar\omega)]\ , \tag{29a}$$
$$f_a^n(E)=\tfrac{1}{2}[f^+(E+n\hbar\omega)-f^-(E+n\hbar\omega)]\ , \tag{29b}$$

and let us call

$$W_n^{f,b}=W_-^{f,b}(E+n\hbar\omega)=W_+^{f,b}[E+(n-1)\hbar\omega)]\ . \tag{30}$$

We obtain the following equations:

$$\frac{d}{dE}f_s^n(E)=-\frac{(1+N_q)}{W_n}f_a^n(E)+N_q\left[\frac{1}{W_n^f}-\frac{1}{W_n^b}\right]f_a^{n-1}(E)-\frac{N_q}{W_{n+1}}f_a^n(E)+(1+N_q)\left[\frac{1}{W_{n+1}^f}-\frac{1}{W_{n+1}^b}\right]f_a^{n+1}(E)\ , \tag{31a}$$

$$\frac{d}{dE}f_a^n(E)=-\frac{1}{W_n}[(1+N_q)f_s^n(E)-N_qf_s^{n-1}(E)]+\frac{1}{W_{n+1}}[(1+N_q)f_s^{n+1}(E)-N_qf_s^n(E)]\ , \tag{31b}$$

with $f_s^{-1}=f_a^{-1}=0$.

This yields the following (exact) sum rules:[22]

$$\frac{d}{dE}\sum_{n=0}^{\infty}f_a^n(E)=0 \text{ or } \sum_{n=0}^{\infty}f_a^n(E)=J=\text{const}\ , \tag{32a}$$

$$\frac{d}{dE}\sum_{n=0}^{\infty}f_s^n(E)=-\sum_{n=0}^{\infty}\left[\frac{1}{W_{n+1}}-\frac{1}{W_{n+1}^f}+\frac{1}{W_{n+1}^b}\right]\times[N_qf_a^n(E)+(1+N_q)f_a^{n+1}(E)]$$
$$=-\sum_{n=0}^{\infty}\frac{2}{W_{n+1}^b}[N_qf_a^n(E)+(1+N_q)f_a^{n+1}(E)]\ , \tag{32b}$$

by using Eqs. (22) and (27). Under moderate or lower fields ($F\leq 500$ V/cm) the electron-phonon interaction is still strong enough to establish a detailed balance between energy intervals so that we can assume

$$N_qf_{a,s}^n(E)=(1+N_q)f_{a,s}^{n+1}(E)\ . \tag{33}$$

We note, in passing, that this equation would be satisfied by a Maxwellian and a linearly "displaced" Maxwellian distribution. However, Eq. (33) with the sum rule (32a) imposes f_a to be constant on each interval so that we obtain

$$f_a^0(E)=\frac{J}{1+N_q}\ . \tag{34}$$

By making use of Eqs. (32a) and (33) we can transform Eq. (32b) and get

$$\frac{d}{dE}\sum_{n=0}^{\infty}\left[\frac{N_q}{1+N_q}\right]^nf_s^0(E)=-\sum_{n=0}^{\infty}\frac{2}{W_{n+1}^b}\left[\frac{N_q}{1+N_q}\right]^{n+1}2J \tag{35}$$

or

$$\frac{d}{dE}f_s^0(E)=-\frac{4JN_q}{(1+N_q)^2}\sum_{n=0}^{\infty}\left[\frac{N_q}{1+N_q}\right]^n\frac{1}{W_{n+1}^b(E)}\ ,$$

where we used

$$1+N_q=\sum_{n=0}^{\infty}\left[\frac{N_q}{1+N_q}\right]^n$$

with

$$N_q=\left[\exp\frac{\hbar\omega}{kT}-1\right]^{-1}\ .$$

The solution $f_s^0(E)$ is then given by

$$f_s^0(E)=f_s^0(0)-\frac{4JN_q}{(1+N_q)^2}\times\sum_{n=0}^{\infty}\left[\frac{N_q}{1+N_q}\right]^n\int_0^E\frac{dE}{W_{n+1}^b(E)}\ , \tag{36a}$$
$$\cong f_s^0(0)-\frac{4JN_q}{(1+N_q)^2}\int_0^E\frac{dE}{W_1^b(E)}\ , \tag{36b}$$

where we dropped the high-order terms of the rapidly convergent n series since

$$\left[\frac{N_q}{1+N_q}\right]^n = e^{-n\hbar\omega/kT}$$

and $1/W^b_{n+1} \ll 1/W^b_1$.

Here $f_s(0)$ is an integration constant which is determined by the condition $f^-(\hbar\omega)=0$ because, in the low-field limit, there is a net depletion of carriers with *negative* momentum just below the POP emission threshold.[12] In this momentum range, the depopulation due to carrier deceleration is not balanced by a corresponding carrier repopulation by POP scattering (Fig. 3). This situation is unique to 1D systems because of the absence of both angular randomization and carrier-carrier scattering, which otherwise would result in a finite population for $p \geq -\sqrt{2m\hbar\omega}$.

Under this condition, f_s becomes

$$f_s(E) = \frac{J}{1+N_q}\left\{1+\gamma\int_{E/\hbar\omega}^1 d\xi\left[1-\left[\frac{\xi}{\xi+1}\right]^{1/2}\right]\times\frac{1}{\sqrt{\xi(\xi+1)}}\right\}$$

$$= \frac{J}{1+N_q}\left\{1+2\gamma\ln\left[1+\frac{\sqrt{2}}{2}\right] - \ln\left[1+\left[\frac{E}{E+\hbar\omega}\right]^{1/2}\right]\right\} \quad (37)$$

with

$$\gamma = 2N_q\hbar\omega/(1+N_q)eFv_c\tau_0$$

and

$$v_c = \sqrt{2\hbar\omega/m} \quad \text{for } 0 \leq E \leq \hbar\omega \ .$$

Here ξ is the integration variable and we have approximated $1/\tau_0^b$ in Eq. (21) by

$$(1/2\tau_0)[1-\sqrt{E/(E+\hbar\omega)}]$$

to fit the energy dependence of the backward-scattering matrix element which is a rapidly decreasing function of energy (Fig. 2 inset). We use Eq. (33) to obtain $f_s(E)$ at high energy $E > \hbar\omega$ and the normalization condition

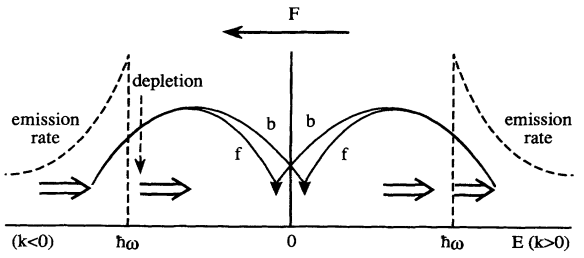

FIG. 3. Schematics of the 1D carrier dynamics in energy space indicating the subthreshold carrier depletion in the negative momentum region. The double arrows represent the carrier drift while the solid line represents the carrier scattering by POP emission. The breakdown of the inversion symmetry $f(t)=f(-k)$ by the electric field is obvious.

$$n_L = \sum_{n=0}^{\infty}\int_0^{\hbar\omega} dE\, D(E+n\hbar\omega) f_s(E+n\hbar\omega)$$

$$= \left[\frac{2m\omega}{\hbar}\right]^{1/2}\frac{J}{\pi(1+N_q)}(A+\gamma B) \ , \quad (38)$$

where $D(E)$ is the 1D density of states, to determine J. Here n_L is the linear carrier concentration, and A and B are coefficients dependent on temperature but independent of field and confinement.

$$A = \frac{2}{1+N_q}\sum_{n=0}^{\infty}\left[\frac{N_q}{1+N_q}\right]^n\sqrt{n+1} \ , \quad (39a)$$

$$B = \sum_{n=0}^{\infty}\left[\frac{N_q}{1+N_q}\right]^n \times\int_0^1\frac{d\xi}{\sqrt{\xi+n}}\int_\xi^1\frac{ds}{\sqrt{s(s+1)}}\times\left[1-\left[\frac{s}{s+1}\right]^{1/2}\right] . \quad (39b)$$

Figure 4 shows the profile of $f_s(E)$ for $F=100$ V/cm, compared with the Monte Carlo simulation (POP scattering only) for the same confinement conditions as in Fig. 2. The agreement is very good except below $E=\hbar\omega$, where the dip in the solid curve is an artifact of the Monte Carlo model which is caused by the quantum broadening of the density of states included in the scattering rates.[23] The distribution function is characterized by "evenly spaced" peaked structures reminiscent of the 1D density of states. This jagged profile in the carrier distribution is naturally possible at high temperature where POP absorption is significant to replicate the peaked structures at multiples of the POP energy $E=n\hbar\omega$. The particular shape of $f_s(E)$ shows that despite the "detailed balance" condition (33) between energy intervals, the Maxwellian distribution is not the solution of Eq. (16). In the limit $F=0$,[24] the distribution function is given by

$$f_0(E) = \frac{\pi}{B}n_L\left[\frac{\hbar}{2m\omega}\right]^{1/2} \times\left\{\ln\left[1+\frac{\sqrt{2}}{2}\right]-\ln\left[1+\left[\frac{E}{E+\hbar\omega}\right]^{1/2}\right]\right\} \quad (40)$$

as a result of Eqs. (37) and (38) in the zero-field limit (for $\gamma\to\infty$ and $J\to 0$). The fact that the latter distribution [Eq. (40)] is not a Maxwellian distribution is a manifestation of the nonergodicity of the 1D system that accommodates a solution different from the Maxwellian at equilibrium. Actually, it is easily verified that the Maxwell-Boltzmann distribution is also a solution of Eqs. (16)–(19) for $F=0$, but this solution is not unique, since any function which satisfies the detailed balance [Eq. (33)] is also a solution of Eqs. (12)–(19). In this respect it should be noticed that our results have been obtained by neglecting all scatterings events except POP scattering. As we mentioned earlier, this situation occurs in practical cases

when $F \gg 10$ V/cm and it is conceivable that at equilibrium ($F=0$) a Maxwellian distribution is established as a result of the combined effects of POP, AP, and II scattering, which rules out the solution (40). At finite fields, however, AP and II scattering become rapidly negligible, and the distribution converges towards the actual profile (Fig. 4). Thus, under the influence of an electric field, the Maxwellian symmetry is more rapidly destroyed than in 2D or 3D systems where the electric field only "displaces" the equilibrium distribution without drastically changing its nature. One can, therefore, regard the onset of this effect as the manifestation of a pronounced organization of the system in the k (momentum) space under the joint influence of the electric field and POP scattering, which drives the electron gas toward a more stable configuration than that given by a Maxwellian profile. This is particularly noticeable if one evaluates the average carrier energy given by

$$\langle E \rangle = \frac{1}{n_L} \sum_{n=0}^{\infty} \int_0^{\hbar\omega} dE\, D(E+n\hbar\omega)(E+n\hbar\omega) \times f_s(E+n\hbar\omega) = \hbar\omega \frac{C+\gamma D}{A+\gamma B} , \quad (41)$$

which is plotted in Fig. 5(a) as a function of electric fields for different temperatures. Here C and D are temperature-dependent coefficients.

$$C = \frac{2}{3} \frac{1}{1+N_q} \sum_{n=0}^{\infty} \left[\frac{N_q}{1+N_q} \right]^n (n+1)^{3/2} , \quad (42a)$$

$$D = \sum_{n=0}^{\infty} \left[\frac{N_q}{1+N_q} \right]^n \times \int_0^1 d\xi \sqrt{\xi+n} \int_{\xi}^1 \frac{ds}{\sqrt{s(s+1)}} \times \left[1 - \left[\frac{s}{s+1} \right]^{1/2} \right] . \quad (42b)$$

It is easily seen that above $T_L = 150$ K, $\langle E \rangle$ is smaller than the thermal energy $kT_L/2$ over an increasing range of electric fields.[25] The big dots are the results of a Monte Carlo simulation which includes the influence of AP scattering at $T_L = 300$ K. The agreement between the two approaches is excellent except for $F < 50$ V/cm where the predominance of AP scattering contributes to heating the system before the transition toward the jagged profile characterized by a low average energy. The figure also shows that the cooling from the thermal energy increases with the temperature, which indicates

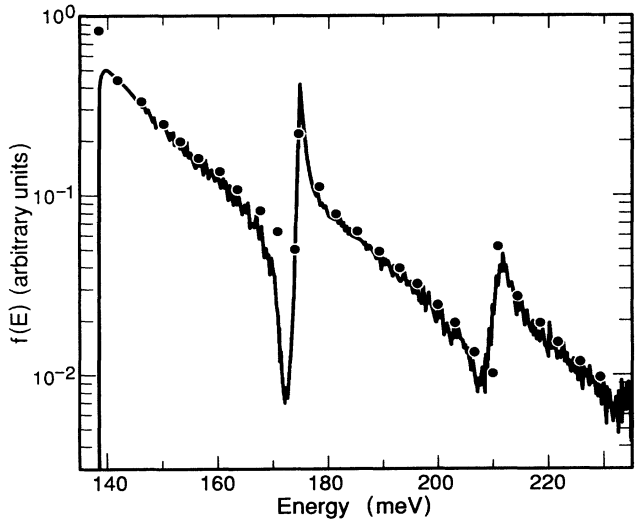

FIG. 4. Energy-distribution function of a single-band 1D electron gas with a longitudinal field $F=100$ V/cm at $T=300$ K. The quantum-wire structure results from confinement in a quantum well with width $L_y = 135$ Å and a triangular potential in a field $F_z = 120$ kV/cm, which places the ground state at 140 meV above the conduction-band edge (Ref. 11). Solid line denotes Monte Carlo simulation dots, which represent the analytic results of Eq. (37).

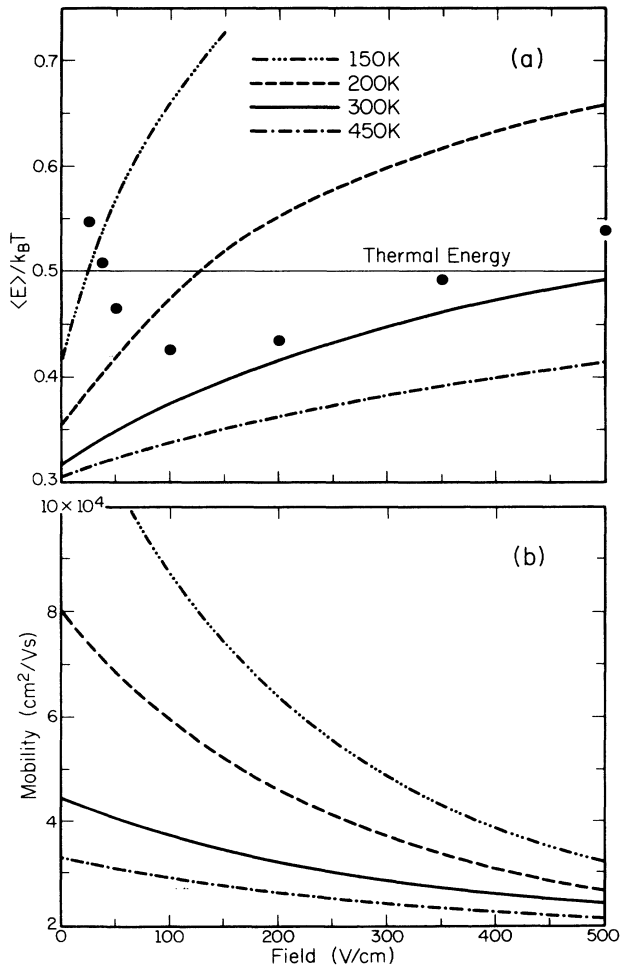

FIG. 5. (a) Average carrier energy as a function of electric fields for four temperatures. Dots denote Monte Carlo simulation with AP and POP scattering at 300 K. Thin lines denote thermal energy $kT/2$. (b) POP mobility for the same temperatures.

the dominant influence of POP absorption. This phenomenon is a high-temperature effect, which is therefore different from the decrease of the thermal (Maxwellian) energy $\langle E \rangle_{\rm Th}$ discussed by previous authors[26–29] and which occurs in 3D systems at low temperature as a result of POP emission processes only. We wish also to point out that the decrease of $\langle E \rangle$ below the thermal energy does not violate Joule heating since the energy gained from the field is directly transferred to the lattice without thermalizing the electron gas in the absence of carrier-carrier collision.

The organization of the distribution into a jagged profile is therefore an increasing function of temperature which occurs *under highly dissipative conditions.* This has important consequences for the transport properties of 1D systems, as seen below. From Eqs. (37) and (38), it is straightforward to calculate the 1D current

$$I = e \sum_{n=0}^{\infty} \int_0^{\hbar\omega} dE\, D(E+n\hbar\omega) v(E+n\hbar\omega) \times f_a(E+n\hbar\omega) = \frac{2eJ\omega}{\pi} , \quad (43)$$

as well as the carrier mobility

$$\mu = \frac{(1+N_q)^2}{B + A\gamma^{-1}} \frac{e}{m} \frac{\tau_0}{N_q} , \quad (44)$$

which is shown as a function of electric field in Fig. 5(b). At high temperature the 1D mobility exceeds the bulk value by a factor of 4 to 5 over a large range of electric fields. For instance, for $F=100$ V/cm at $T=300$ K, Eq. (44) yields $\mu \sim 3.8\times10^4$ cm^2/V s (Monte Carlo simulation yields $\mu=3\times10^4$ cm^2/V s with both POP and AP scattering[11]) which is several times larger than the bulk value ($\mu=8\times10^3$ cm^2/V s). This high value results from the fact that the distribution function only depends on the backward-scattering rate $(1/\tau^b)$ [Eq. (36)], which is much weaker than the f rate (Fig. 2 inset). In this transport process controlled by strong POP emission and absorption, the 1D thermal energy is converted into a drift motion of carriers which boosts the mobility. From Fig. 5(b), it can be seen that this effect also increases with temperature, contrary to bulk or 2D transport.

In conclusion, we want to emphasize that the cooling effect and the mobility enhancement are unique features of 1D transport at high temperature which manifests the absence of ergodicity in the electron system. Specifically, phonon absorption is the important process which is responsible for the existence of jagged structures in the distribution and results in improved transport performances. From a general standpoint, the structures in the distribution function are relatively robust and persist in multiband systems where the basic features of this effect contribute to enhanced POP-assisted intersubband resonances similar to the magneto-phonon effect, and set on population inversion between subbands.[14,15]

ACKNOWLEDGMENTS

The author would like to thank S. Briggs and D. Jovanovic for fruitful discussions. He is indebted to Mrs. C. Willms and G. Miller for technical assistance. This work is supported by the Joint Service Electronic Program and the National Center for Computational Electronics at the University of Illinois.

[1]P. Petroff, A. Gossard, R. Logan, and W. Wiegmann, Appl. Phys. Lett. **41**, 635 (1982).
[2]A. Warren, D. Antoniadis, and H. Smith, Phys. Rev. Lett. **56**, 1858 (1986).
[3]K. Kash, A. Scherer, J. Worlock, H. Craighead, and M. Tamargo, Appl. Phys. Lett. **49**, 1043 (1986).
[4]T. Hiramoto, K. Hirakawa, Y. Iye, and T. Ikoma, Appl. Phys. Lett. **51**, 1620 (1987).
[5]M. Tsuchiya, J. M. Gaines, R. H. Yan, R. J. Simes, P. O. Holtz, L. A. Colden, and P. M. Petroff, Phys. Rev. Lett. **62**, 466 (1989).
[6]E. Colas, E. Kapon, S. Simhony, H. M. Cox, R. Bhat, K. Kash, and P. S. D. Lin, Appl. Phys. Lett. **55**, 867 (1989).
[7]For a review see, e.g., *Nanostructure Physics and Fabrication* edited by M. A. Reed and W. P. Kirk (Academic, New York, 1989).
[8]J. P. Leburton and D. Jovanovic, Semicond. Sci. Technol. (to be published).
[9]H. Sakaki, Jpn. J. Appl. Phys. **19**, L735 (1980).
[10]H. Sakaki, in *Proceedings of the Ninth International Symposium on GaAs and Related Compounds, Oiso, Japan, 1981,* edited by T. Sugano (IOP, Bristol, 1982), p. 251.
[11]S. Briggs and J. P. Leburton, Phys. Rev. B **38**, 8163 (1988).
[12]S. Briggs and J. P. Leburton, Phys. Rev. B **39**, 8025 (1989).
[13]J. P. Leburton, S. Briggs, and D. Jovanovic, Superlatt. Microstruct. **8**, 209 (1990).
[14]S. Briggs and J. P. Leburton, Superlatt. Microstruct. **5**, 145 (1989).
[15]S. Briggs, D. Jovanovic, and J. P. Leburton, Appl. Phys. Lett. **54**, 2012 (1989).
[16]See, e.g., K. Hess, in *Physics of Non-Linear Transport in Semiconductors,* edited by D. K. Ferry, J. R. Barker, and C. Jacoboni (Plenum, New York, 1980).
[17]S. Briggs (unpublished).
[18]C. Kittel, *Quantum Theory of Solids* (Wiley, New York, 1987).
[19]H. Fröhlich, H. Pelzer, and S. Zienau, Philos. Mag. **41**, 221 (1950).
[20]M. Stroscio, Phys. Rev. B **40**, 6428 (1989).
[21]This point was brought to my attention by P. Kocevar.
[22]These sum rules are relatively general; similar results for spatially nonhomogeneous transport have been obtained by Mahan *et al.* for optic-deformation-potential phonon scattering; see, e.g., G. D. Mahan, J. Appl. Phys. **58**, 2242 (1985); G. D. Mahan and G. S. Canright, Phys. Rev. B **35**, 4365 (1987).
[23]S. Briggs, B. A. Mason, and J. P. Leburton, Phys. Rev. B **40**, 1200 (1989).
[24]K. Hess, Phys. Rev. B **10**, 3374 (1974).
[25]Without loss of generality we can assume the electron concen-

tration is weak enough ($n_L \lesssim 10^6$/cm) and does not change the phonon temperature during the process.
[26]V. V. Paranjape and T. P. Ambrose, Phys. Lett. **8**, 223 (1964).
[27]Z. S. Gribnikov and V. A. Kochelap, Zh. Eksp. Teor. Fiz. **58**, 1046 (1970) [Sov. Phys. JETP **31**, 562 (1970)].
[28]R. L. Peterson, Phys. Rev. B **2**, 4135 (1970).
[29]L. E. Vorobev, V. S. Komissarov, and V. I. Stafev, Fiz. Tekh. Poluprovodn. **7**, 88 (1973) [Sov. Phys. Semicond. **7**, 59 (1973)].